MARS CLIMATE SOUNDER OBSERVATIONS OF WAVE STRUCTURE IN THE NORTH POLAR MIDDLE ATMOSPHERE OF MARS DURING THE SUMMER SEASON. Paulina Wolkenberg[1] and R. J. Wilson[2], [1]Centrum Badań Kosmicznych Polska Akademia Nauk, paulina@cbk.waw.pl, [2]NOAA Geophysical Fluid Dynamics Laboratory, Princeton, New Jersey, USA, john.wilson@noaa.gov.

Introduction: Our study is based on observations from the Mars Climate Sounder (MCS) [1] aboard the Mars Reconnaissance Orbiter (MRO) spacecraft [2]. The temperature field was retrieved from the observations with possible errors of 0.5 – 2 K for all altitudes [3]. The vertical range of the temperature profiles is from 5 – 10 km above the surface up to 80 - 90 km. We examine the temperature field at over a full range of heights and latitudes during the northern summers of Mars Years 28-31. We make a selection of temperature field for daytime and nighttime data around LT = 1500 and LT = 0300, respectively. Then we have calculated the difference temperature field from $(T_{3pm} - T_{3am})/2$ and the averaged temperature field from $(T_{3pm} + T_{3am})/2$ from 85°S to 85°N in 5 degree latitude bins, zonally and in time averaged at each 10 of Ls. The T-average and T-difference fields are applied to find Fourier components and identify the presence of non-migrating, migrating and stationary waves during MY 29, 30 and 31.

In a local solar time reference frame, which is appropriate for spacecraft observations from sun-synchronous orbits (MGS, MRO), the longitude-time dependence is given as:

$$A(\lambda, t_{LT}) \sim \Sigma A_{s,\sigma} \cos[\, (s-\sigma)\lambda + \sigma t_{LT} - \delta_{s,\sigma}\,]$$

An observed zonal wave m variation can reflect the combined presence of a stationary wave, $A_{m,\,0}$ and a set of nonmigrating tides with $A_{s,\sigma}$, such that $(s - \sigma) = \pm m$ [4],[5].

Fig. 1 presents a mixture of non-migrating, migrating and stationary waves. In the south hemisphere stationary waves with the m = 1 zonal component are evident between 60°S to 80°S extending from the surface to 1 Pa. The semidiurnal zonal symmetric tides contribute mainly to the m = 2 zonal component between 60°N and 80°N at around 0.1 Pa. Amplitudes around 5 K are more prominent at L_s = 105° than for subsequent L_s intervals. The T-average field for the m = 3 zonal component contains the semidiurnal eastward propagating tide with s= 1 (SE1), the semidiurnal westward propagating tide with s= 5 (SW5) and stationary waves. However, the T avg and T diff fields are not sufficient to resolve amplitudes of individual tide components. In particular, only 2x/sol data, it was not previously possible to identify the semi-diurnal tide and distinguish the semi-diurnal tide from a stationary wave in the T-average field. Therefore, we make use of MCS observations employing cross-track viewing in addition to the usual along-track viewing, as described in [6]. The resulting multi-track data, which provide observations at 6-7 local times per sol, allow us to distinguish eastward and westward propagating diurnal waves and identify semidiurnal tides [6]. In order to resolve particular tides we fit the multi-track observations to the diurnal and semi-diurnal temporal harmonics. Thus the new MCS observations (cross-track) allows a fitting of the $A_{s,\sigma}$ coefficients to the data.

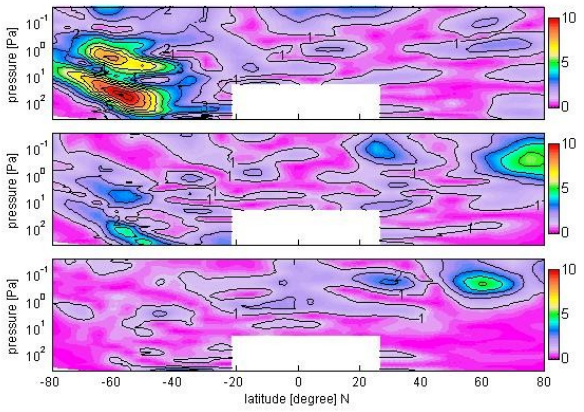

Figure 1. T-average field from L_s = 100° to L_s = 110° and for m=1 (top), m=2 (middle) and m=3 (bottom) for three MYs together. The interval in contour is 1 K.

We have explored the strength and persistence of observed wave-1, wave-2, and wave-3 structures as a function of latitude, altitude, and season. We note three temperature maxima, forming a well-defined wave-3 structure in the middle atmosphere, during each of our 3 Mars years at the same season (L_s = 100° - 110°) at around 0.1 Pa (~70 km) over the northern polar region of Mars from 50°N to 90°N (Fig.2a). Fourier analysis is employed to find the amplitudes and phases of the various wave components as a function of latitude, altitude, and season.

During the L_s = 0–135° season we have found weak inter-annual variability in temperature (Fig.2b), thus we have composited the data in blocks in 5 of latitude degrees from 85°S to 85°N, in the 10 of longitude degrees and in the 10 of Ls degrees for three Mar-

tian years from MY 29 to 31 together. After L_s = 135° there was early-season dust lifting in MY 29.

We use the MY31 MCS multi-track data to show that these waves are not stationary, but have diurnal and semi-diurnal components. These measurements began in September 2010 (MY30, L_s = 144) and have been carried out in 30 sols on, 30-sols off sequences since then. The period of most relevance for this study is L_s = 101 - 114 in MY31 (Fig.2c). Fig. 2c presents temperature variations from the multi-scan (cross-track and along-track) data with time and zonal mean removed. From the least-square fitting in time (2 harmonics) and space (4-6 waves) to the data we can clearly obtain amplitudes and phases of the individual components of the total wave field.

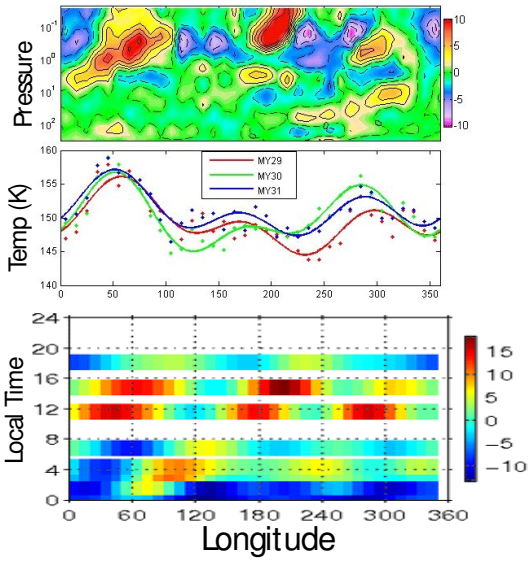

Figure.2a (top) Composite T_{3pm} field at 60-65°N as a function of longitude and pressure during L_s = 100-110°. The contour interval is 2 K. **2b**. (middle) Zonal variation of T_{3pm} at 1 Pa for three MYs during L_s = 100-110° and at 60-65°N. **2c**. (bottom) Zonal variation of T with the zonal mean removed at 0.1 Pa and at 57.5-62.5°N during L_s = 101° - 114°. The longitude scale is the same for all three panels.

Results: By using the increased local time coverage provided by the the multi-scan data we are able to distinguish the contributions of the individual tide modes. After detail analysis of multi-track data from L_s = 101° – 114° at 0.1 Pa we found that the main contribution to the temperature field is from the migrating diurnal and semidiurnal tides (m=0). The westward propagating diurnal tide (DW1) has an amplitude for 8-10 K while the semidiurnal migrating tide (SW2) has an amplitude of 5.5 K at 55°N – 60°N and which decreases to 2.2 K at 60°N – 65°N, in accord with [6].

Amplitudes of the diurnal eastward nonmigrating tide with s = 1 (DE1) increase up to 4.1 K northward which constitute the component of T-difference for m = 2. Contrary to the DE1, the semidiurnal eastward propagating tides with s = 1 (SE1) decreases northward achieving a ~2 K amplitude at 60° - 65°N. The tide contributes to the T-average field and is mainly responsible for the m = 3 zonal component in Figure 1. Amplitudes around 4 K for this tide were found at 55° - 60°N which is in an agreement with Fig.1. Their intensity decreases with latitude according to Fig.1. The diurnal eastward tide (DE2) exhibits the same behavior with latitude, which comprises the T-difference field for m = 3. It is worth noting that the semidiurnal zonally symmetric tides with amplitude around 4.3 K is also important in the T-average field for m = 2 and it was not previously discernible from stationary waves (Fig.1). However, the wave 2 component of T-average dominates that of T-difference, as it is appropriate for a semidiurnal tide. Thus, the m = 2 wave structure is due to contributions from the zonally symmetric semidiurnal tide ($A_{0,2}$) and the diurnal eastward tide, $A_{-1,1}$ while the m = 3 structure is due to diurnal eastward propagating tide ($A_{-2,1}$) and semidiurnal eastward tide ($A_{-1,2}$) that had been suggested by previous modeling and observational studies [7], [8], [9]. Together, they sum to a significant temperature variation. The results are in general accord with MGCM simulations, which will also be shown. We will discuss the seasonal variation of these waves and how that may relate to the evolving zonal state of the atmosphere.

References:

[1] McCleese, D. J., et al. (2007), *J. Geophys. Res*., 112, E05S06, doi:10.1029/2006JE002790.

[2] Zurek, R. W., and S. E. Smrekar (2007) *J. Geophys. Res*., 112, E05S01, doi:10.1029/2006JE002701.

[3] Kleinböhl , A., et al. (2009) *J. Geophys. Res*., 114, E10006, doi: 10.1029/2009JE003358.

[4] Banfield, D. et al. (2003) *Icarus*, 161, 319–345.

[5] Wilson, R. J. (2000) *Geophys. Res. Lett*., 27, 3889–3892.

[6] Kleinböhl, A., et al. (2013) *Geophys. Res. Lett., 40*, doi:10.1002/grl.50497. [

[7] Wilson, R. J. (2002) *Geophys. Res. Lett.*, 29 (7), 10.1029/2001GL013975.

[8] Angelats i Coll, M. et al. (2004) *J. Geophys. Res.*, 109, E01011, doi:10.1029/2003JE002163.

[9] Bougher, S. W., et al. (2001) *Geophys. Res. Lett*., 28, 3091–3094.